

Computer simulation of the spreading of metallic clusters landing at grazing incidence on a metallic surface

F. J. Palacios, M. P. Iñiguez, M. J. López, and J. A. Alonso

Departamento de Física Teórica, Universidad de Valladolid, 47011 Valladolid, Spain

(Received 19 April 2000)

Simulations of the impact of metallic clusters at grazing incidence on a metallic surface are presented. The interatomic interactions are described by a many-body potential rooted on the tight-binding formalism. Several molecular dynamics simulations are performed to study the influence of some relevant parameters such as the initial velocity, the chemical identities of the cluster and the surface and the nature of the surface plane. For the velocities studied here (10–54 Å/ps) a soft cluster landing at grazing incidence on a hard metal surface simply spreads over the surface without causing much damage and the degree of spreading depends on the initial cluster velocity. A channeling effect occurs when the cluster moves originally in a direction parallel to atomic channels on the surface. On the other hand a hard cluster landing on a soft metallic surface can penetrate into the substrate material and the degree of fragmentation also depends on the initial velocity.

I. INTRODUCTION

A number of theoretical studies of cluster deposition on solid surfaces involving metallic materials have been performed in recent years.^{1–6} Motivation for these studies comes from the interest in nanofabrication methods and in possible technological applications of the nanostructured surfaces obtained upon cluster deposition. Typically these clusters are formed by a few tens, hundreds, or thousands of atoms. This method is very suitable in such applications as surface or thin-film growth because the clusters release their energy in a region localized near the surface and do not penetrate deeply into the bulk. The structure and properties of the thin films formed depend on the details of the cluster deposition.⁷ The supported structures obtained from cluster deposition can be observed experimentally by means of atomic force and scanning tunnelling microscopies and have interest for future nanoscale electronic applications.⁸ Other applications such as surface cleaning or sputtering have also a technological potential in very large scale integrated processing.⁹

We present a computer-simulation study of the deposition of metallic clusters landing at grazing incidence on a metal surface. The interest of studying nonperpendicular impact is highlighted by recent work by van Dijken, *et al.*¹⁰ These authors have studied the deposition of atomic Cu beams on Cu(001) surfaces at incident angles that deviate strongly from the usual perpendicular incidence (deviations between 50° and 85°). The results reported show striking differences with respect to those obtained in the same work for perpendicular deposition. The importance of oblique impact in cluster deposition was stressed by Moseler, *et al.*,¹¹ who have shown, using molecular-dynamics and mesoscopic modeling, that impact onto a tilted part of the substrate surface is responsible for the observed surface smoothing by energetic cluster impact. But to our knowledge, investigations of the grazing impact of clusters are still lacking. In our simulations the clusters are initially very close to the surface (within the interaction range of the cluster-surface potential) and have a

component of the velocity parallel to the surface. Several molecular-dynamics (MD) simulations are performed to determine the influence of different factors on the deposition process: the initial cluster velocity, the surface orientation, and the chemical nature of cluster and surface atoms. To model the interatomic interactions a semiempirical many-body potential derived from the tight-binding method is used.¹² The simulation method is briefly described in Sec. II and the results are shown and discussed in Sec. III. The influence of the impact velocity is analyzed for Au₅₅ landing on a Cu(011) surface. Comparison of the results with those obtained for Al₅₅ on Ni(011), Ni₅₅ on Al(011), Ni₅₅ on Ni(011) and Al₅₅ on Al(011) serves to analyze the effect of chemical nature of cluster and substrate. Some simulations for impact of Al₅₅ on a Ni(001) surface allow us to study the influence of surface plane orientation. A different kind of cluster motion on a surface, arising from purely thermal effects, has been studied experimentally and theoretically in other works,^{2,13–16} and unexpected diffusion mechanisms have been discovered.

II. MODEL

In this paper the clusters and substrate surfaces involve the metallic elements Ni, Al, Cu, and Au. The clusters are initially near the surface within the interaction range of the cluster-surface potential. To model the interatomic interactions, we use a semiempirical many-body potential derived from the tight-binding method,^{17,18} that for a system containing N atoms of the same element is

$$V = \frac{1}{2} \sum_{i=1}^N \left[\sum_{j=1}^N A e^{-p(r_{ij}/r_0-1)} - \left(\sum_{j=1}^N \xi^2 e^{-2q(r_{ij}/r_0-1)} \right)^{1/2} \right] \quad (1)$$

with $j \neq i$. The first term is a repulsive pair potential and the second is an attractive many-body band-energy contribution. r_{ij} is the distance between atoms i and j and r_0 is a reference distance, usually the equilibrium nearest neighbor distance in

the bulk metal. The values of these parameters are fitted to reproduce the magnitude of bulk equilibrium cohesive properties. The generalization to two types of atoms is straightforward¹⁹ and the corresponding parameters are fitted to the cohesive properties of crystalline solid alloys. The values of the parameters for the materials used in this paper are given in Ref. 20. A cutoff radius for the potential is introduced such that interactions up to fifth nearest neighbors enter the simulation. In the case of heteroatomic interactions the cutoff chosen is the larger of the two different radii.

The substrate is modeled by a crystalline parallelepipedic block with fcc structure. The surface is in the (x, y) plane and periodic boundary conditions are imposed in the x and y directions. The substrate is formed by three types of atomic layers: several top layers whose atoms are treated by constant energy MD, a single thermal layer whose function is to dissipate the excess thermal energy that the impinging cluster releases to the substrate during landing, and three inert bottom layers formed by fixed atoms that serve to compute forces on the atoms inside the nonstatic layers. The atoms of the intermediate thermal layer obey the Nose-Hoover equations,^{21,22} which contain a friction term, and in this way the substrate is coupled to a heat bath. The substrate block has between five thousand and ten thousand atoms and typical dimensions are $4 \times y \times 2$ nm, where y varies in the range 6–20 nm. This means that we have about ten layers in the direction perpendicular to the surface (including also thermal and inert layers) and that the block is long enough in the initial direction of motion of the cluster, the y direction. Two different surface plane orientations have been studied: (011) and (001). To focus on the effect of cluster velocity and to separate this from thermal effects due to the temperature of the substrate,²³ the substrate is initially thermalized at $T = 0$ K, and the effect of the thermal layer is to ensure that the temperature of the whole system after deposition would also be $T = 0$ K after equilibration following a transient time.

The clusters landing on the metallic surfaces are icosahedral 55-atom clusters whose structure and interatomic distances have been previously optimized by an steepest-descent method by starting from an ideal Mackay icosahedron.²⁴ The clusters are initially placed near the surface such that the minimum distance between a cluster atom and the top atomic layer is 3.5 Å. This distance is a little larger than typical bulk interatomic distances in these materials, which vary in the range 2.5–2.9 Å, but at the same time is short enough to allow the cluster to interact with the substrate. Initially, a velocity parallel to the surface is given to the cluster. That velocity ranges between 10 and 54 Å/ps. With those velocities we achieve cluster kinetic energies in the KeV range, typical of impact deposition.^{1–4,25} Since at the beginning of the simulation the velocity in the direction perpendicular to the surface is zero, the cluster impacts the substrate with a velocity component in the perpendicular direction due only to the cluster-substrate interaction potential. This velocity is small so the landing is at near grazing incidence. The use of an optimized icosahedral cluster structure is a convenient assumption since icosahedral structures are rather common for metallic clusters.²⁶ According to density-functional calculations by Garzón *et al.*,²⁷ the lowest-energy structure of Au₅₅ is disordered, but the icosahedral isomer is

only 0.011 eV above. A number of experiments and theoretical calculations support the icosahedral structure of Ni₅₅.²⁶ Density-functional calculations by Yi *et al.*²⁸ predict that a cuboctahedral fcc structure is more stable than the icosahedral one for Al₅₅, but that structure is also compact and rather spherical. In practice the use of icosahedral isomers does not bias our conclusions since the clusters dismember and spread during the impact process.

To monitor the impact of the cluster on the substrate we use several indicators. The evolution of the y and z coordinates of the center-of-mass of the cluster, y_{cm} and z_{cm} , respectively, reflect well the characteristic time scales of the main atomic rearrangements occurring in the impact process. In this respect, and for the purposes of calculating the coordinates of the center-of-mass, all the atoms initially in the cluster are taken into account, even if the cluster dismembers and loses its identity during landing. Another indicator, that gives information on the evolution of the shape of the cluster, is an elongation parameter defined as

$$\epsilon = \frac{\sum_{i=1}^N |y_i - y_{cm}|}{\sum_{i=1}^N |x_i - x_{cm}|} \quad (2)$$

whose value is larger than 1.0 for clusters with an elongated shape in the y direction. ϵ is the ratio of the average y and x coordinates of the atom positions with respect to the center-of-mass of the cluster, and consequently this parameter gives no information about the shape in the z direction, perpendicular to the surface.

III. RESULTS

A. Time scale of the impact process and influence of the initial cluster velocity

The characteristic time scales of the phenomena occurring when the cluster lands on the surface at near grazing incidence are reflected in Fig. 1, where z_{cm} and y_{cm} , the z and y coordinates of the center-of-mass of the cluster, are plotted for the case of a Au₅₅ cluster initially moving parallel to the channels in the $[01\bar{1}]$ direction on a Cu(011) surface with an initial velocity component parallel to the surface $v_p = 10$ Å/ps [Fig. 1(a)] and $v_p = 20$ Å/ps [Fig. 1(b)]. Those surface channels can be seen in Fig. 2. At the beginning of the simulation y_{cm} varies linearly with t , that corresponds to the free flight period before touching the surface. During this free flight the velocity component perpendicular to the surface, arising solely from the cluster-substrate interaction is about 1 Å/ps. But at a time $t_i = 5$ ps, y_{cm} experiences a drastic deceleration and this time can be taken as the instant of impact of the cluster with the surface. At this time, cluster bonds start breaking and new bonds form between cluster and surface atoms. A second characteristic time t_s can be noticed at which y_{cm} does not change any more. This is the stopping time. t_s is close to 8 ps for the simulation of Fig. 1(a) and about 10 ps in Fig. 1(b), as a consequence of the higher initial kinetic energy of the cluster in the second simulation. That is, $t_s - t_i = 3$ ps and 5 ps, respectively, in Figs. 1(a) and 1(b). Those two characteristic times t_i and t_s

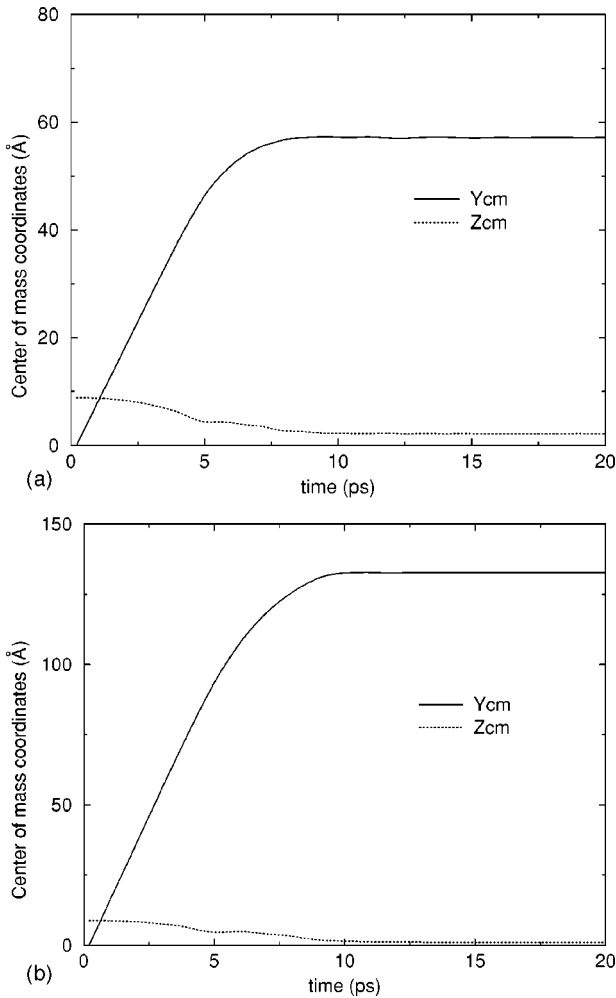


FIG. 1. Time evolution of the y and z coordinates of the center-of-mass of Au_{55} landing on a $\text{Cu}(011)$ surface with initial parallel velocities $v_p = 10$ Å/ps (a) and $v_p = 20$ Å/ps (b).

are also reflected in features in z_{cm} : the slope of z_{cm} has a break at t_i and z_{cm} reaches a constant value at t_s . In the interval between t_i and t_s , z_{cm} gives a measure of the flattening of the cluster.

The effect of the initial cluster velocity on the shape of the deposited cluster is drastic: the configurations of the cluster after stopping ($t=20$ ps) are shown in Fig. 2. In the case of lower v_p the cluster still forms a connected body, although heavily distorted and flattened. However, for $v_p = 20$ Å/ps the cluster becomes spread and fragmented along the direction of motion. It now forms a flat disconnected strip. A few Cu atoms have been displaced from their original positions leaving vacancies behind, and most of those vacancies have been filled by Au atoms, replacing the original Cu atoms. A quantitative measure of the spreading is given by the ϵ parameter defined in Eq. (2). Its evolution with time is given in Fig. 3. ϵ changes fast in the interval (t_i, t_s) and reaches a practically constant value after t_s .

B. Influence of the chemical nature of cluster and substrate

To analyze the influence of the chemical identity of cluster and substrate we compare the results for Au-Cu with results for simulations for the system Al-Ni, and for the ho-

moatomic cases Ni-Ni and Al-Al. Previous studies of vertical cluster impact deposition for the Al-Ni system have shown great differences when the chemical natures of the cluster and substrate are interchanged.¹ Figure 4 shows the results of two simulations for Al_{55} landing on a $\text{Ni}(011)$ surface with initial cluster velocities $v_p = 20$ Å/ps and $v_p = 54$ Å/ps, respectively. The impact time, $t_i = 1$ ps, is lower than for the noble metals of Fig. 1. This is a consequence of the higher force exerted by a more attractive cluster-substrate interaction in the Al-Ni case. A more attractive interaction is expected from theories of alloy formation²⁹ and also from the existence of intermetallic compounds with high melting temperatures in the Al-Ni system as compared to Cu-Au.³⁰ The elapsed time between impact and stopping is also smaller. In summary, the stopping interval Δt appears to be determined by the magnitude of the attractive interaction (or tendency to form alloys) between cluster and substrate elements. Again, as in the case of Au-Cu, the shape of the cluster after stopping depends on v_p . Figures 5 and 6 show snapshots at $t = 20$ ps for the simulations with $v_p = 54$ Å/ps and with $v_p = 20$ Å/ps, respectively. Those shapes are completely different. The cluster has a planar connected shape for the lower v_p but it is completely dismembered and spread out in the case of the higher v_p . This becomes reflected in the values of the parameter ϵ plotted in Fig. 7. ϵ is larger for $v_p = 54$ Å/ps. Figures 2(b) and 6 show very different results, yet the initial velocity was $v_p = 20$ Å/ps in both cases. The gold cluster dismembers completely on the Cu surface while the Al cluster flattens but remains as a connected body on the Ni surface. Two factors contribute to the different behavior. First, the kinetic energy of the Al atoms is lower due to their lower mass, and second the more attractive Al-Ni interaction is more effective in reducing the spreading of the Al cluster. In the configuration of Fig. 5 one appreciates [see also Fig. 2(b)] that some substrate atoms have been removed from their original positions in the outermost substrate layer and have been replaced by Al atoms.

A strikingly different behavior is observed when the role of Al and Ni are interchanged, that is when a Ni cluster impacts on an Al surface. We have simulated the impact of Ni_{55} on an $\text{Al}(011)$ surface for initial cluster velocities $v_p = 20$ Å/ps and $v_p = 54$ Å/ps. The feature seen in the snapshots of Fig. 8, that correspond to $v_p = 20$ Å/ps, is the substantial damage produced in the substrate as soon as the Ni cluster impacts on the Al surface. This damage occurs because the substrate is a soft metal compared to the projectile. In fact, the melting temperature $T_m(\text{Al}) = 932$ K is nearly one-half of that of Ni, $T_m(\text{Ni}) = 1725$ K. Then we observe that a hard projectile (Ni_{55}) causes great damage on the surface of a soft substrate (Al) while a soft projectile (Al_{55}) does not cause appreciable damage on a hard metal surface (only displacements of some of the outermost surface atoms). The value of ϵ after stopping remains close to 1.2, and the snapshot at $t = 20$ ps gives the explanation: the hard cluster becomes partially embedded into the Al matrix but it remains fairly compact. The cluster removes a substantial amount of Al atoms from the surface and near-surface layers and some of those atoms partially cover the Ni cluster. The melting temperatures of Au and Cu are nearly identical [$T_m(\text{Cu}) = 1357$ K, $T_m(\text{Au}) = 1336$ K], so being equally hard, it becomes understandable that the Cu surface remains

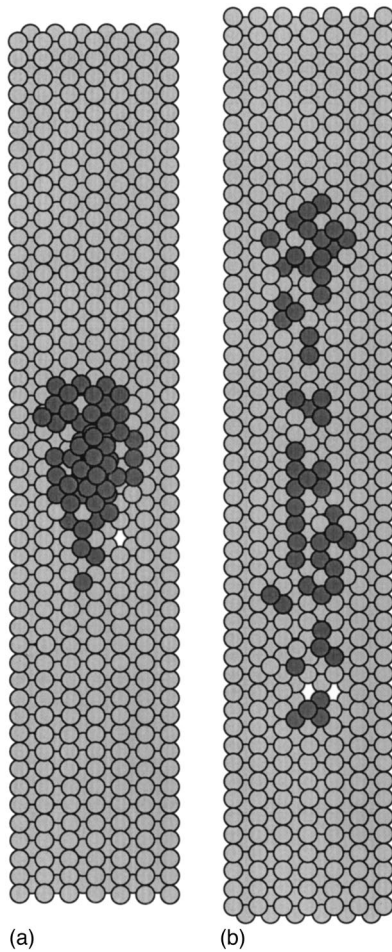


FIG. 2. Shape of the Au_{55} cluster after stopping (20 ps) for the two simulations of Fig 1. (a) $v_p = 10 \text{ \AA/ps}$, and (b) $v_p = 20 \text{ \AA/ps}$.

nearly undamaged. In perpendicular cluster impact a crater is formed on the surface^{11,31} but we find no crater formation in the case of grazing incidence. Between all the cluster-surface combinations studied here, the case just described, that is, the impact of Ni_{55} on the Al surface, is the only one that produces a structure with a mild resemblance to the formation of a crater on the substrate. This arises from the combination of a hard cluster and a soft substrate. Nevertheless, as one can appreciate in Fig. 8, the crater has been filled by the cluster.

Increasing v_p to 54 \AA/ps also produces interesting results. Snapshots given in Fig. 9 for $t = 3 \text{ ps}$, $t = 10 \text{ ps}$, and $t = 20 \text{ ps}$ show a higher damage and also partial dismembering of the cluster, that loses atoms as it penetrates into the substrate. A fraction of the transient disorder seen at $t = 3 \text{ ps}$ anneals out later on, and at $t = 20 \text{ ps}$ the picture obtained is that of a surface region with some vacancies, but the lattice itself has recovered well its crystalline face-centered-cubic structure in the region of impact. The Ni_{55} cluster has lost a number of atoms although it seems to retain a core of connected Ni atoms at the end of the simulation. At that time ϵ is near 3. The atoms lost by the travelling cluster are not well mixed with the host. Those Ni atoms form several dimers. Our interpretation is that this reflects the negligible solid solubility of Ni in bulk Al.³² Although Ni and Al form crystal compounds NiAl_3 , Ni_2Al_3 , NiAl , and Ni_3Al , the conditions for producing such compounds are evidently

not met in our simulation. In particular, an adequate substrate temperature that would promote thermal diffusion of atoms would be required. The heat released during impact to the substrate is enough to allow for the local atomic rearrangements that anneal a large part of the topological lattice disorder, reverting the lattice to a state with a good degree of crystallinity, but is not enough to promote the long-range diffusion that would allow ordered compound formation.

Simulations for homoatomic systems give complementary information. Figure 10 shows snapshots for the landing of Ni_{55} on a $\text{Ni}(011)$ surface with (a) $v_p = 20 \text{ \AA/ps}$ and (b) $v_p = 54 \text{ \AA/ps}$. The snapshots are taken at 20 ps, and the different colors distinguish cluster and substrate atoms. In case (a) there is no damage on the substrate and the cluster forms a rather flat epitaxial island with ϵ near 1.2. This is a consequence of the identical nature of cluster and substrate. The cluster dismembers completely in case (b), and a few surface vacancies is the only damage produced. A similar behavior is observed for Al_{55} landing on $\text{Al}(011)$ at $v_p = 54 \text{ \AA/ps}$, Fig. 10(c), but with a slightly higher damage on the substrate, that appears as a consequence of the Al substrate softness. In summary, at the impact velocities studied here, we confirm that the substrate is appreciably damaged only when the cluster is substantially harder than the substrate.

A more quantitative analysis of the damage caused in the substrate by the cluster impact as well as of the final structure of the combined system formed by the substrate and the deposited cluster is presented in Table I. The number of substrate atoms (N_S^r) which are kicked out from their original positions in the substrate and that move to positions above the substrate surface, increases with v_p , is larger in the heteroatomic cases than in the homoatomic cases, and is larger for harder clusters. For the homoatomic cases and for a soft cluster landing on a hard surface (i.e., Al on Ni), the removed substrate atoms adopt epitaxial positions with respect to the substrate surface and most of the empty places left out in the substrate by the removed atoms are filled in by cluster atoms. The net effect is a very small number of vacancies in the substrate. Most cluster atoms do not insert into the substrate and adopt epitaxial positions above the substrate surface. In the case of a hard cluster landing on a soft substrate (i.e., Ni on Al) more than half of the cluster atoms penetrate into the substrate. For the initial cluster velocity $v_p = 20 \text{ \AA/ps}$ the cluster remains quite compact and does not create vacancies into the substrate. The cluster atoms do not adopt positions corresponding to the substrate lattice and, consequently, the Al atoms that partially cover the Ni cluster are not in epitaxial configurations with respect to the substrate surface either. For the initial cluster velocity $v_p = 54 \text{ \AA/ps}$ the picture is quite different. Most (43 out of 47) of the cluster atoms that penetrate onto the substrate adopt final positions corresponding to lattice points of the substrate. Moreover a big number of vacancies are left out on the substrate upon cluster impact. A significant fraction of the substrate atoms that move above the substrate surface are not able to adopt epitaxial configurations with respect to the surface substrate. The idea that the outcome of the impact depends crucially on the ratio of the cohesive energies (hardnesses) of cluster and substrate materials (and on the cluster kinetic energy) was first introduced by Hsie *et al.*,¹ in their

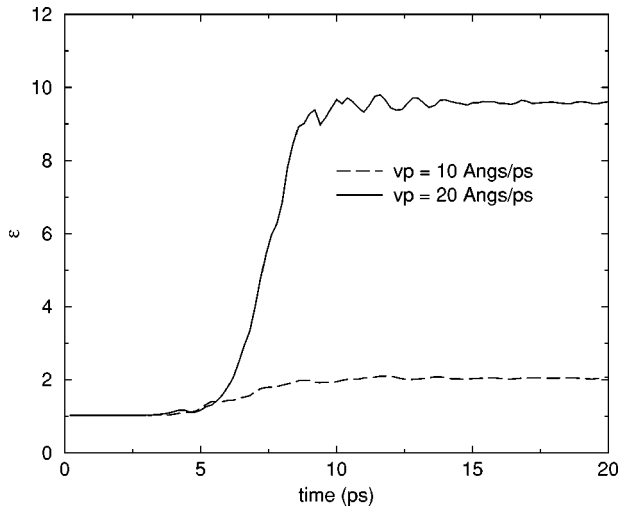


FIG. 3. Time evolution of the shape parameter ϵ of Au_{55} for the two simulations of Fig. 1.

molecular-dynamics simulations of perpendicular cluster impact. We conclude that the same variables control the outcome of grazing impact.

Moseler *et al.*¹¹ have simulated the impact of large Cu clusters (1000–2000 atoms) on a tilted Cu surface. The tilt

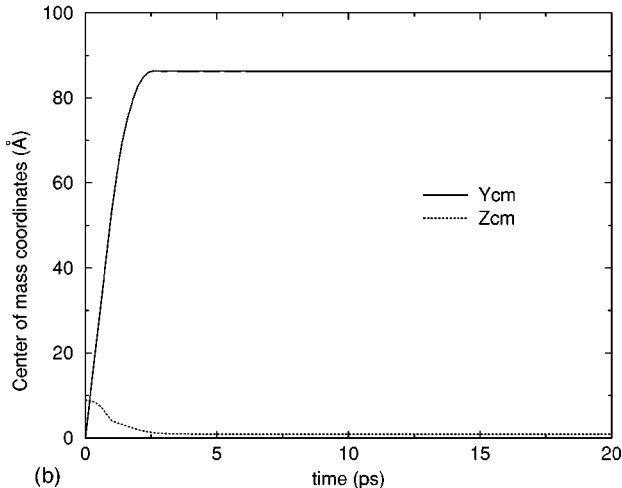
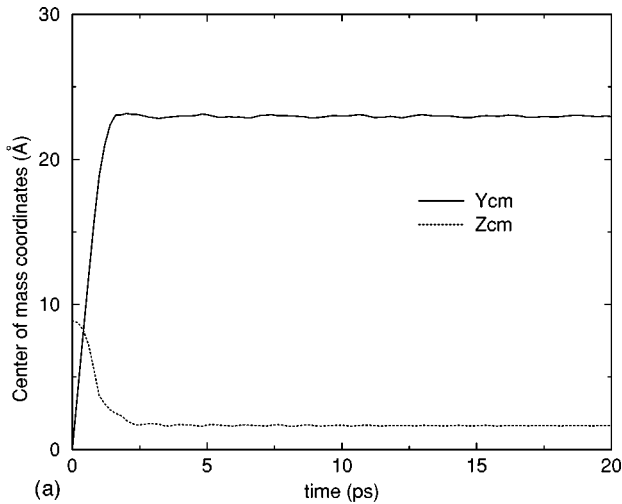


FIG. 4. Time evolution of the y and z coordinates of the center-of-mass of Al_{55} landing on a $\text{Ni}(011)$ surface with initial parallel velocities $v_p = 20$ Å/ps (a) and $v_p = 54$ Å/ps (b).

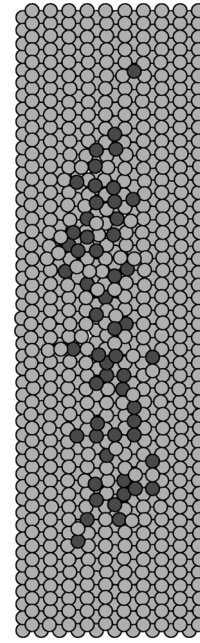


FIG. 5. Shape of the Al_{55} cluster landing on $\text{Ni}(011)$ after stopping ($t = 20$ ps) for an initial cluster velocity $v_p = 54$ Å/ps.

angle, that is the angle between the direction of incidence and the direction normal to the surface, was smaller than 10° . In our simulations the clusters are smaller and the tilt angle is much larger (larger than 80°). But the initial kinetic energies of the incident clusters are in the range of KeV's in both series of simulations and useful contact between them can be established. Moseler *et al.*, find that the tilt angle has the effect of inducing a downhill particle current that reduces the local roughness initially produced by the cluster impact. In our simulations the mass transport, that is the spreading of the cluster in the y direction seen in Fig. 2, is a trivial consequence of the large tilt angle. The mass transport was quantified by Moseler by defining the displacement sum

$$\delta_N = \sum_i d^{(i)}, \quad (3)$$

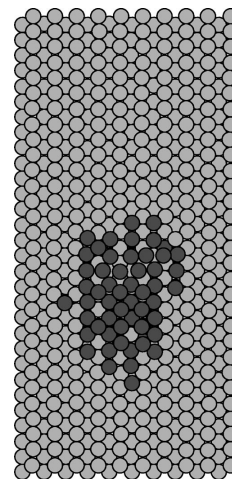


FIG. 6. Shape of the Al_{55} cluster landing on $\text{Ni}(011)$ after stopping ($t = 20$ ps) for an initial cluster velocity $v_p = 20$ Å/ps.

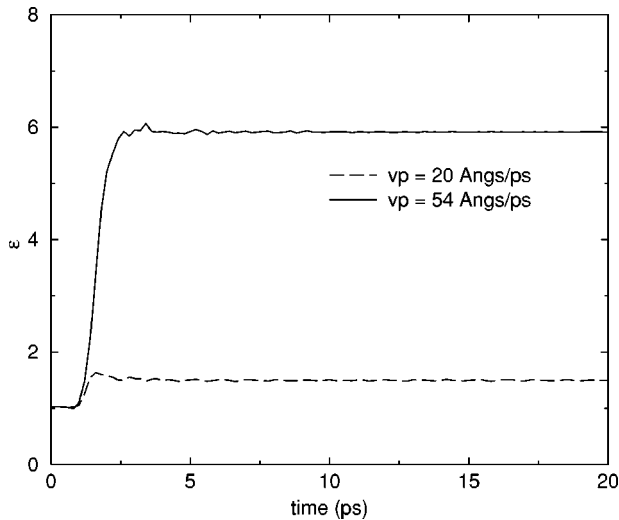


FIG. 7. Time evolution of the shape parameter ϵ of Al_{55} for the two simulations of Fig. 4.

where $d^{(i)}$ is the displacement of atom i along the direction of the slope, and the sum is extended over the N atoms of the cluster. An empirical law

$$\delta_N \propto NE^{1/2} \quad (4)$$

was discovered, relating δ_N and the impact energy of the cluster E . We have data for simulation of Al_{55} landing on $\text{Ni}(011)$ at four different kinetic energies. The analysis of the displacements suggests a law linear in E , namely,

$$\delta_N \propto NE. \quad (5)$$

The difference should not be surprising, and we ascribe it to the very different tilt angles in our simulations compared to those in Moseler's work.

The results obtained in this section and in Sec. III A above involve the impact of icosahedral 55-atom clusters. For some metallic elements, especially the transition metals, the closed-shell icosahedral structure makes this cluster size more stable than clusters of neighbor sizes²⁶ and the question arises of the generality of our results. However the binding energies vary slowly with cluster size in the size range of several dozen atoms and the differences in binding energy per atom between clusters that are not too similar are in the order of 0.01 eV only. These differences are small compared to the kinetic energies of the impacting clusters, so we can safely predict that similar results will be obtained for other clusters with a few tens of atoms.

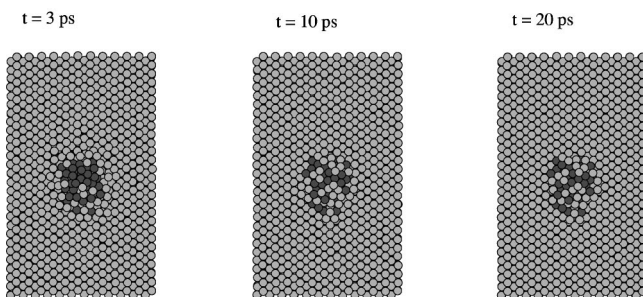


FIG. 8. Snapshots at 3 ps, 10 ps, and 20 ps for Ni_{55} landing on an $\text{Al}(011)$ surface with initial parallel velocity $v_p = 20$ Å/ps.

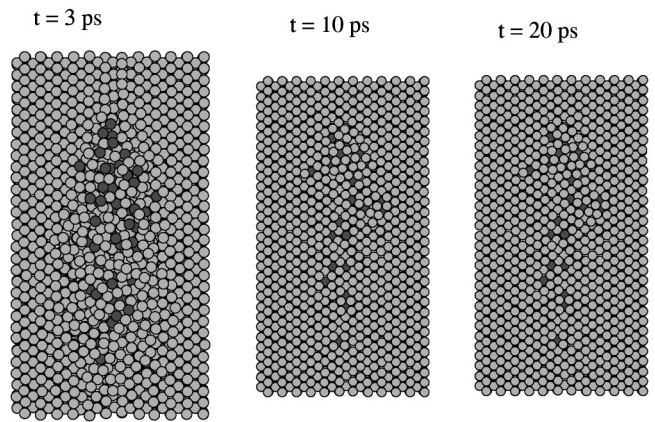


FIG. 9. Snapshots at 3 ps, 10 ps, and 20 ps for the landing of Ni_{55} on an $\text{Al}(011)$ surface with initial velocity $v_p = 54$ Å/ps.

C. Influence of the surface plane orientation. Channeling effect

To study the effect of the nature of the surface plane on the deposition process we compare the impact of an Al_{55} cluster on a Ni surface in two different orientations (011) and (001). Those surfaces are shown in Fig. 11. Atoms that are part of the outermost surface plane are represented by dark spheres and the light-gray spheres represent atoms in the next atomic plane. The nearest-neighbor distance in the fcc crystal is given as r_0 and the lattice constant is $a_0 = \sqrt{2} r_0$. For each surface, two different directions of cluster motion have been selected. In the case of the (011) surface the motion directions are $[01\bar{1}]$ and $[100]$. Those directions are indicated in Fig. 11(a). For the (001) surface the directions selected are $[110]$ and $[100]$, indicated in Fig. 11(b). The initial cluster velocity was in all cases $v_p = 54$ Å/ps.

The general features of the impact deposition are similar in all cases, that is the cluster dismembers and spreads over the surface, but some subtle differences occur during the stopping interval. Table II gives the values of the elongation parameter ϵ after stopping. The largest value, $\epsilon = 6.0$ occurs for motion along the $[01\bar{1}]$ direction on the (011) surface. Lower values occur for motion along the $[100]$ direction on the same surface (case B) and along the $[110]$ direction on the (001) surface (case C), with the smallest value of ϵ , namely, $\epsilon = 2.9$, for the motion along the $[100]$ direction on the (001) surface (case D). The explanation for the differ-

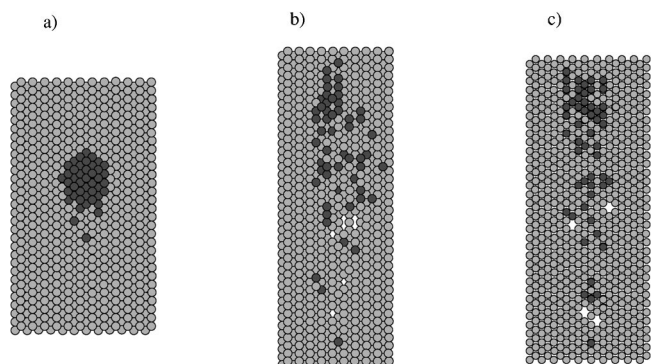


FIG. 10. Snapshots at 20 ps for (a) the landing of Ni_{55} on $\text{Ni}(011)$ with initial velocity $v_p = 20$ Å/ps and (b) with $v_p = 54$ Å/ps; (c) the landing of Al_{55} on $\text{Al}(011)$ with initial velocity $v_p = 54$ Å/ps.

TABLE I. Some characteristics of the cluster-substrate final configuration upon cluster deposition at near grazing incidence with initial parallel velocity v_p (in $\text{\AA}/\text{ps}$). N_S^r is the number of substrate atoms that move above the substrate surface, either in epitaxial positions (N_S^e) or in non epitaxial positions (N_S^{ne}) with respect to the substrate surface. N_S^v is the number of vacancies in the substrate. N_C^i , N_C^e , and N_C^{ne} are the number of cluster atoms that penetrate into the substrate, sit on the substrate surface at epitaxial positions, and sit on the substrate surface at nonepitaxial positions, respectively.

Cluster	Substrate	v_p	N_S^r	N_S^e	N_S^{ne}	N_S^v	N_C^i	N_C^e	N_C^{ne}
Al	Al	54	16	16	0	4	12	43	0
Ni	Ni	20	6	6	0	0	6	49	0
Ni	Ni	54	19	19	0	7	12	42	1
Al	Ni	20	2	2	0	0	2	48	5
Al	Ni	54	23	18	5	5	18	32	5
Ni	Al	20	30	8	22	0	34	1	20
Ni	Al	54	90	57	33	43	47	2	6

ences in ϵ appears to be a channeling effect, that is, the focused motion of atoms along the atomic channels in the surface. The width of the channels is $a_0 = \sqrt{2}r_0$ in case A, r_0 in cases B and C, and $a_0/2 = r_0/\sqrt{2}$ in case D. One can observe a correlation between the value of ϵ and the width of the atomic channel. Channels of r_0 or lower are rather narrow and it is reasonable to obtain a reduced elongation ϵ compared to case A, because the higher channel width facilitates the focused motion of the atoms.

When the velocity is reduced to $v_p = 20 \text{ \AA}/\text{ps}$, the Al cluster impacting on the Ni(001) surface forms an island similar to the case of the Ni(011) surface. In summary, only when the kinetic energy is high enough and the cluster dismembers and there are isolated Al atoms moving on the surface, the channeling mechanism becomes effective.

In their simulations of perpendicular impact of Cu clusters on a Cu surface, Nordiek *et al.*³¹ found that the shape and size of the crater formed on the substrate depends on the

surface orientation. The variations were attributed to the different shear constants along different crystallographic directions. Those differences enhance particle transport along certain directions and justify the elongated crater shapes obtained for certain surface orientations. To this interesting result we now can add another mechanism for particle transport, namely, surface channeling. By its very nature this mechanism is probably important only in the cases of grazing incidence of clusters or atoms. It should be interesting to investigate if any relative atomic size conditions are required for its occurrence.

IV. CONCLUSIONS AND COMMENTS

The behavior of metallic clusters landing at grazing incidence on metallic surfaces has been studied by computer simulation using many-body interaction potentials rooted on tight-binding theory. The size of the clusters was always 55 atoms, and the variety of combinations of cluster and substrate covers the whole range of possibilities: (a) the cluster is a metal of larger cohesive energy than the substrate (Ni on Al), (b) the cluster has a lower cohesive energy than the substrate (Al on Ni), (c) cluster and substrate have similar cohesive energies (Au on Cu), and (d) cluster and substrate are identical metals (Ni on Ni; Al on Al). The effect of the initial velocity of the incident cluster was also studied. In the range of velocities studied here, 10 to 54 $\text{\AA}/\text{ps}$, the grazing impact produces a total or a partial dismembering of the cluster and the precise behavior depends on two ingredients: the kinetic energy of the cluster and the relative cohesive energies of cluster and substrate metals. When the cluster is softer than the substrate, that is, if the cluster has a lower cohesive energy, or if both have similar cohesive energies, the cluster simply flattens and forms a planar island when the incident velocity is low, and it becomes partially or completely dismembered if the velocity is larger. In both cases the cluster becomes at rest in a few picoseconds and the atoms remain on the surface, removing a few surface atoms and producing a few surface vacancies, some of these filled

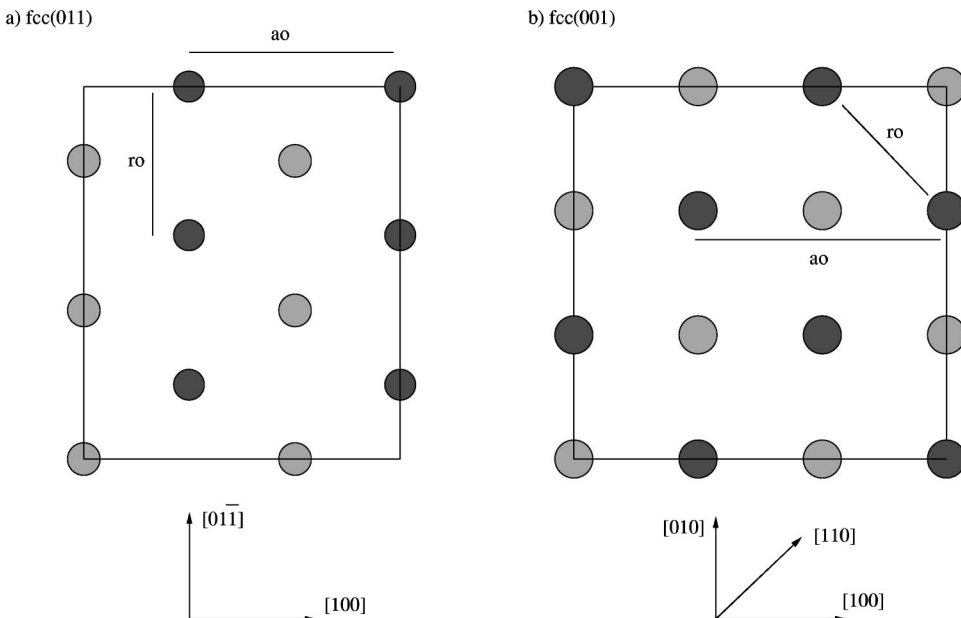


FIG. 11. Structure of the fcc (001) and fcc (011) surfaces.

TABLE II. Elongation parameter ϵ for an Al_{55} cluster landing on a Ni surface for different directions of cluster motion, and width W of the corresponding surface channels.

Surface	Direction	ϵ	W
011	$[01\bar{1}]$	6.0	$\sqrt{2}r_0$
011	$[100]$	3.2	r_0
001	$[100]$	2.9	$r_0/\sqrt{2}$
001	$[110]$	3.8	r_0

by the cluster atoms, but the amount of damage done on the substrate surface remains very small. In contrast, a ‘‘hard’’ cluster shows a rather different behavior. At an incident velocity of 20 Å/ps, a Ni_{55} cluster landing on an Al surface penetrates in part into the substrate and some of the atoms removed cover the cluster, which does not show appreciable fragmentation. On the other hand, by increasing the incident velocity to 54 Å/ps the cluster fragments heavily and causes larger damage, as it penetrates into the substrate, although a part of the damage anneals out by the time the cluster atoms come to rest. By comparing the results for Al_{55} landing on two different surface planes of Ni [the (011) and (001) surface orientations, respectively] we have observed a channelling effect when the direction of incidence is parallel to one of surface channels. This channelling effect enhances the spreading of the cluster.

The simulations described in this paper have been performed at a very low substrate temperature (ideally 0 K) to suppress thermal diffusion and to concentrate on the localized effects due to the cluster impact. A finite substrate temperature will certainly add interesting new effects³³ to those found here. Room temperature is well suited to produce thin films by cluster impact techniques.^{3,7–9} In these techniques

the activation energies for lateral atomic displacements are provided by the cluster velocity, in contrast to substrate heating in the conventional atomic vapor deposition. In a previous work²³ we studied the influence of the substrate temperature on the soft landing of Cu_{55} and Au_{55} clusters on Cu(001). The results showed that heating the substrate produces a progressive flattening of the deposited clusters. However, there are only minor differences for different temperatures up to 800 K during the first 10 ps of the process, that is, for times of the order of the stopping time encountered here. Obviously, the later evolution of the deposited structures for longer times will be affected by thermal diffusion.

In the usual cluster deposition experiments the clusters impact the surface travelling in the perpendicular direction. In practice the focusing may not be perfect and clusters may impact with a slightly different angle. Also the surface may be tilted on a nanoscopic scale. Moseler *et al.*¹¹ have shown that the impact on a tilted part of the substrate induces a downhill particle current responsible for the smoothing of the surface roughness observed at a mesoscopic scale. A tilting of only 5°–10° seems to be enough to produce the observed smoothing. Our simulations correspond to an extreme case of tilting and predict that the deposition of clusters at grazing incidence can provide a useful way to develop nanostructures at the nanoscopic scale. A careful selection of materials and velocities may lead to a controlled patterned covering of metallic surfaces with low substrate damage.

ACKNOWLEDGMENTS

Work supported by DGES (Grants PB98-0345 and PB98-0368). M.J.L. acknowledges support from Universidad de Valladolid.

-
- ¹H. Hsie, R.S. Averback, H. Sellers, and C.P. Flynn, *Phys. Rev. B* **45**, 4417 (1992).
- ²W.D. Luedtke and U. Landman, *Phys. Rev. Lett.* **82**, 3835 (1999).
- ³H. Haberland, M. Mall, M. Moseler, Y. Qiang, T. Reinert, and Y. Thurner, *J. Vac. Sci. Technol. A* **12**, 2925 (1994).
- ⁴L. Rongwu, P. Zhengying, and H. Yukun, *Phys. Rev. B* **53**, 4156 (1996).
- ⁵C. Massobrio and B. Nacer, *Z. Phys. D* **40**, 526 (1996).
- ⁶G. Betz and W. Husinsky, *Nucl. Instrum. Methods Phys. Res. B* **122**, 311 (1997).
- ⁷H. Haberland, Z. Insepov, and M. Moseler, *Phys. Rev. B* **51**, 11 061 (1995).
- ⁸R.P. Andres, J.D. Bielefeld, J.I. Henderson, D.B. James, V.R. Kolagunta, C.P. Kubiak, W.J. Mahoney, and R.G. Osifchin, *Science* **273**, 1690 (1996).
- ⁹W. Mahoney, D.M. Schaefer, A. Patil, R.P. Andres, and R. Reifengerger, *Surf. Sci.* **316**, 383 (1994).
- ¹⁰S. van Dijken, L.C. Jorritsma, and B. Poelsema, *Phys. Rev. B* **61**, 14 047 (2000).
- ¹¹M. Moseler, O. Rattunde, J. Nordiek, and H. Haberland, *Nucl. Instrum. Methods Phys. Res. B* **164-165**, 522 (2000).
- ¹²F.J. Palacios, M.P. Ñiguez, M.J. López, and J.A. Alonso, *Comput. Mater. Sci.* **17**, 515 (2000).
- ¹³S.C. Wang and G. Ehrlich, *Phys. Rev. Lett.* **79**, 4234 (1997).
- ¹⁴S.C. Wang, U. Kürpick, and G. Ehrlich, *Phys. Rev. Lett.* **81**, 4923 (1998).
- ¹⁵J.M. Wen, S.L. Chang, J.W. Burnett, J.W. Evans, and P.A. Thiel, *Phys. Rev. Lett.* **73**, 2591 (1993).
- ¹⁶W. Fan, X.G. Gong, and W.M. Lan, *Phys. Rev. B* **60**, 10 727 (1999).
- ¹⁷F. Ducastelle, *J. Phys. (France)* **31**, 1055 (1970).
- ¹⁸R.P. Gupta, *Phys. Rev. B* **23**, 6265 (1981).
- ¹⁹M.J. López, P.A. Marcos, and J.A. Alonso, *J. Chem. Phys.* **104**, 1056 (1996).
- ²⁰F. Cleri and V. Rosato, *Phys. Rev. B* **48**, 22 (1993).
- ²¹S. Nose, *J. Chem. Phys.* **81**, 511 (1984).
- ²²W.G. Hoover, *Phys. Rev. A* **31**, 1695 (1985).
- ²³F.J. Palacios, M.P. Ñiguez, M.J. López, and J.A. Alonso, *Phys. Rev. B* **60**, 2908 (1999).
- ²⁴A.L. Mackay, *Acta Crystallogr.* **15**, 916 (1962).
- ²⁵I. Yamada, *Appl. Surf. Sci.* **43**, 23 (1989).
- ²⁶J.A. Alonso, *Chem. Rev.* **100**, 637 (2000).
- ²⁷I.L. Garzón, K. Michaelian, M.R. Beltrán, A. Posada-Amarillas,

- P. Ordejon, E. Artacho, D. Sanchez-Portal, and J.M. Soler, *Phys. Rev. Lett.* **81**, 1600 (1998).
- ²⁸J.Y. Yi, D.J. Oh, J. Bernholc, and R. Car, *Chem. Phys. Lett.* **174**, 461 (1990).
- ²⁹A.K. Niessen, F.R. de Boer, R. Boom, P.F. de Châtel, and W.C.M. Mattens, *CALPHAD: Comput. Coupling Phase Diagrams Thermochem.* **7**, 51 (1983).
- ³⁰R. Hulgren, P.R. Desai, D.T. Hawkins, M. Gleiser, and K.K. Kelley, *Selected Values of Thermodynamic Properties of Binary Alloys* (American Society for Metals, Metals Park, OH, 1973).
- ³¹J. Nordiek, M. Moseler, and H. Haberland, *Radiat. Eff. Defects Solids* **142**, 27 (1997).
- ³²F.R. de Boer, R. Boom, W.C.M. Mattens, A.R. Miedema, and A.K. Niessen, *Cohesion in Metals* (Transition Metal Alloys, North Holland, Amsterdam, 1988).
- ³³W.D. Luedtke and U. Landman, *Phys. Rev. Lett.* **73**, 569 (1994); C.L. Cleveland and U. Landman, *Science* **257**, 355 (1992).